

Engineered Defects for Investigation of Laser- Induced Damage of Fused Silica

A. V. Hamza, et al.

This article was submitted to XXXIII Annual Symposium on Optical
Materials for High Powered Laser – Boulder Damage Symposium,
Boulder, Colorado, October 1-3, 2001

December 18, 2001

U.S. Department of Energy

Lawrence
Livermore
National
Laboratory

This document was prepared as an account of work sponsored by an agency of the United States Government. Neither the United States Government nor the University of California nor any of their employees, makes any warranty, express or implied, or assumes any legal liability or responsibility for the accuracy, completeness, or usefulness of any information, apparatus, product, or process disclosed, or represents that its use would not infringe privately owned rights. Reference herein to any specific commercial product, process, or service by trade name, trademark, manufacturer, or otherwise, does not necessarily constitute or imply its endorsement, recommendation, or favoring by the United States Government or the University of California. The views and opinions of authors expressed herein do not necessarily state or reflect those of the United States Government or the University of California, and shall not be used for advertising or product endorsement purposes.

This work was performed under the auspices of the U.S. Department of Energy by University of California, Lawrence Livermore National Laboratory under Contract W-7405-Eng-48.

Engineered defects for investigation of laser-induced damage of fused silica at 355nm

A. V. Hamza^{a*}, W. J. Siekhaus^a, A. M. Rubenchik^a, M. Feit^a, L.L. Chase^a,
M. Savina^b, M. J. Pellin^b, I. D. Hutcheon^a, M. C. Nostrand^a, M. Runkel^a,
B. W. Choi^a, M. Staggs^a, and M. J. Fluss^a

^aUniversity of California, Lawrence Livermore National Laboratory,
Livermore, CA 94551 USA

^bArgonne National Laboratory, 9700 S. Cass Avenue, Argonne, IL 60439 USA

ABSTRACT

Embedded gold and mechanical deformation in silica were used to investigate initiation of laser-induced damage at 355-nm (7.6 ns). The nanoparticle-covered surfaces were coated with between 0 and 500 nm of SiO₂ by e-beam deposition. The threshold for observable damage and initiation site morphology for these “engineered” surfaces was determined. The gold nanoparticle coated surfaces with 500nm SiO₂ coating exhibited pinpoint damage threshold of <0.7 J/cm² determined by light scattering and Nomarski microscopy. The gold nanoparticle coated surfaces with the 100nm SiO₂ coatings exhibited what nominally appeared to be film exfoliation damage threshold of 19 J/cm² via light scattering and Nomarski microscopy. With atomic force microscopy pinholes could be detected at fluences greater than 7 J/cm² and blisters at fluences greater than 3 J/cm² on the 100 nm-coated surfaces. A series of mechanical indents and scratches were made in the fused silica substrates using a nano-indenter. Plastic deformation without cracking led to damage thresholds of ~25 J/cm², whereas indents and scratches with cracking led to damage thresholds of only ~5 J/cm². Particularly illuminating was the deterministic damage of scratches at the deepest end of the scratch, as if the scratch acted as a waveguide.

Keywords: Nanoparticles, Controlled indentations, Controlled scratches, Laser-induced damage at 355 nm

INTRODUCTION

The laser-induced damage threshold of the surface of a fused silica optic is much lower than the dielectric breakdown threshold of pure bulk fused silica. Extrinsic factors such as scratches and/or impurities limit the performance of the optic¹⁻³. Fortunately, optics manufacturers are improving their optics at a rapid pace. So much so that finding the extrinsic factor before damage occurs is becoming next to impossible. In presently available fused silica optics the number of extrinsic damage sites at 12 J/cm² at 3-ns pulse length at 355-nm wavelength is less than 0.1/cm² [see paper by Menapace *et al.* in this issue]. In order to provide well-defined input and validation to laser-surface damage models⁴, we have produced fused silica optical surfaces with engineered defects that could be well-characterized before and after laser photon interaction at 355 nm. Both impurities in and mechanical insults to the optic were engineered. Gold nanoparticles were chosen as impurity particles for incorporation into optical surfaces because they are available in very narrow size distributions. Indents and scratches were produced by a pyramidal diamond-tipped nano-indenter.

Gold nanoparticle impurities in silica have been previously produced, characterized, and their interaction with laser photons studied⁵. In the previous work the particles were smaller than those used here and, also, had a broader size distribution. The variation in gold nanoparticle sizes led to less deterministic damage events and to damage features that could not be easily detected even with atomic force microscopy.

* Correspondence: Email: Hamza1@llnl.gov, Telephone: 925 423 9198

Scratches on surfaces have also been previously studied¹⁻³. For example, the work of Genin and co-workers¹ showed the cracks were facile damage initiators. However, by controlling the crack formation quantitative information of the damage properties of known loads may be determined.

2.0 EXPERIMENT

2.1 Gold Nanoparticle Sample Preparation

Samples were produced to provide 355-nm laser damage characteristics for known defects in silica. Gold colloidal particles in a proprietary solution were purchased. Particle sizes are 20, 40, and 60 nm. HF etched 2" flats (supplied by SESO) were used as substrates. A siloxane surfactant was used to keep the Au particle from agglomerating on the substrate. The particle density produced was ~ 0.1 particles per μm^2 for the 60nm Au particles (see figure 1). Particle size and density was measured by atomic force microscopy (AFM). The substrates with gold particles were coated with a 100nm (on side 1) and 500nm (on side 2) SiO_2 layer deposited by e-beam evaporation. A schematic of the finished optic is shown in figure 2. The coating covered the 60nm particles; however, at the particle the coating protrudes above the smooth surface by the same 60nm. The width of the protrusion is larger due to the coating process. These Au particle samples were damage tested at LLNL with the Zeus Laser facility.

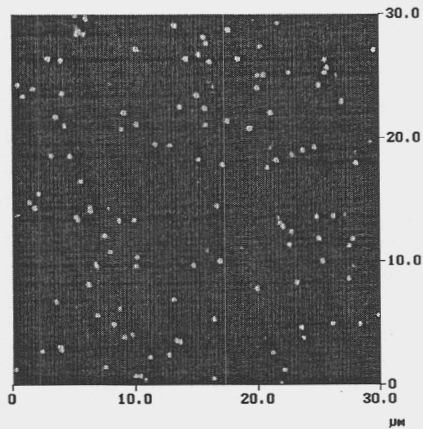


Figure 1. AFM image of 60 nm Au particles deposited on etched 2" SESO part.

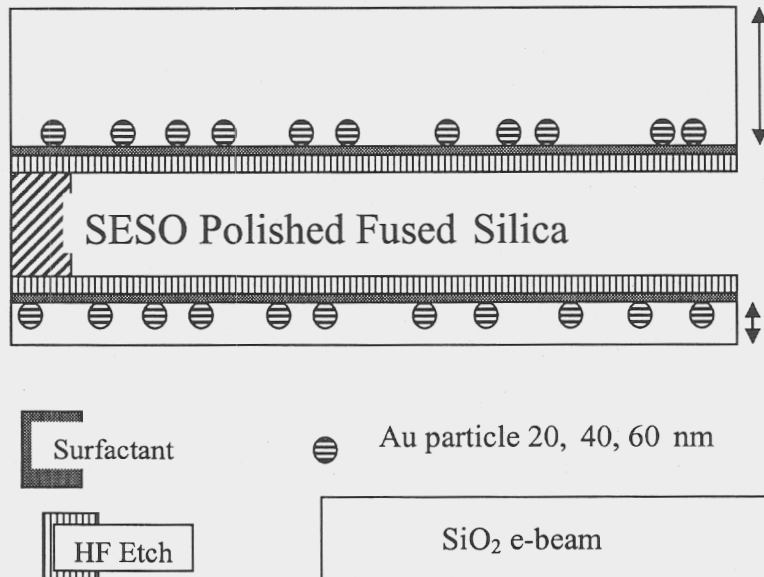


Figure 2. Schematic of engineered Au particle samples. The SiO_2 overcoat was 500nm on side 1 and 100nm on side 2.

Identical samples (1.8 x 1.8 x 1 cm) were produced for time-of-flight (TOF) mass analysis of the 355-nm laser ablated material. The TOF was performed at Argonne National Laboratory's Charisma facility⁶. Measurements were performed with the existing Argonne desorption laser (1- μ m beam spot, 355 nm, 15 ns, 1-2 μ m depth of field) and a diode-induced Nd:YAG (DiNY) laser (30 x 60 μ m beam spot, 60 degree from normal angle of incidence, 355-nm, 6 ns, 2mm depth of field). Post Ionization was available with either a F₂ or a Ti:Sapphire laser. The F₂ laser parameters were 2 mJ at 157 nm and 7 ns pulse length and repetition rate of 700 Hz. The Ti:Sapphire laser pulse length was 40 ns and repetition rate was 1 kHz. The Si resonance transition was 3P₀ \rightarrow 3D₀ at 220.868 nm (2nd harmonic, ~25 mJ) + 441.736 nm to ionize (3rd harmonic of the same fundamental, ~150 mJ). The gold resonance transition was 2S \rightarrow 2P₀ at 267.674 nm (3rd harmonic, ~40 mJ), plus a second 267.674 nm photon to ionize.

2.2 Mechanically Damaged Sample Preparation

Samples were produced to provide 355-nm laser damage characteristics for known mechanical defects in silica. HF etched 2" flats (supplied by SESO) were used as substrates. Mechanical indents and scratches were made in the fused silica substrates using a nano-indenter. The nano-indenter used a triangular pyramid-diamond tip to produce both the indents and scratches. A series of indents (16 each) were made for 0.1, 0.5, 1, 2, 5, 10, and 13 μ m in depth. The applied load and depth were monitored during both loading and unloading for each indent (see figure 3). The indents were characterized by optical microscopy (all) and atomic force microscopy (0.5 μ m and 0.1 μ m indents).

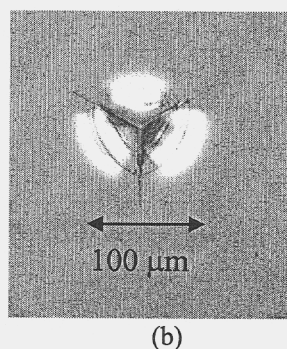
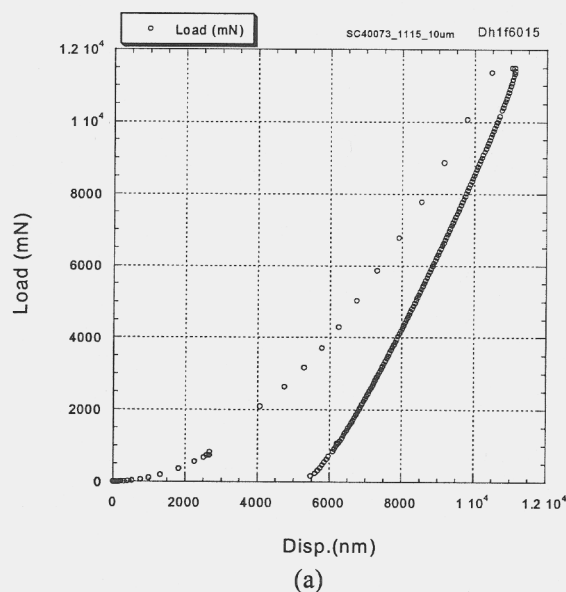


Figure 3. (a) Loading and unloading data for a 10 μ m indent with the Nano-indenter. (b) Optical micrograph of indent.

A series of scratches (16) was made with depth of 0.1, 0.5, 1, and 2 μ m. Three more scratches were made with 5 μ m depth. Scratches were 500 μ m long with the depth tapered from zero depth to the labeled depth at the end of the scratch. Scratches were done "point on", i. e. by dragging the indenter in the direction of one of the pyramid edges. The applied load and depth were monitored during scratching and the depth of the scratch was also profiled before and after scratching (see figure 4). The scratches were also characterized by optical microscopy (all) and atomic force microscopy (0.1, 0.5 and 1 μ m depths).

The difference in the before and after profiles illustrates the densification of the silica in the scratch and indent regions. Under pressure during the indentation and scratch the silica deforms to depth set by the nanoindenter. After the indenter is removed some of the densification is removed; however, some of the densification remains as evidenced by the plastically deformed region. During the scratching process it cannot be ruled out that some of the material may be removed by "plowing." However, no removed material is observed via atomic force microscopy, thus making some densification likely.

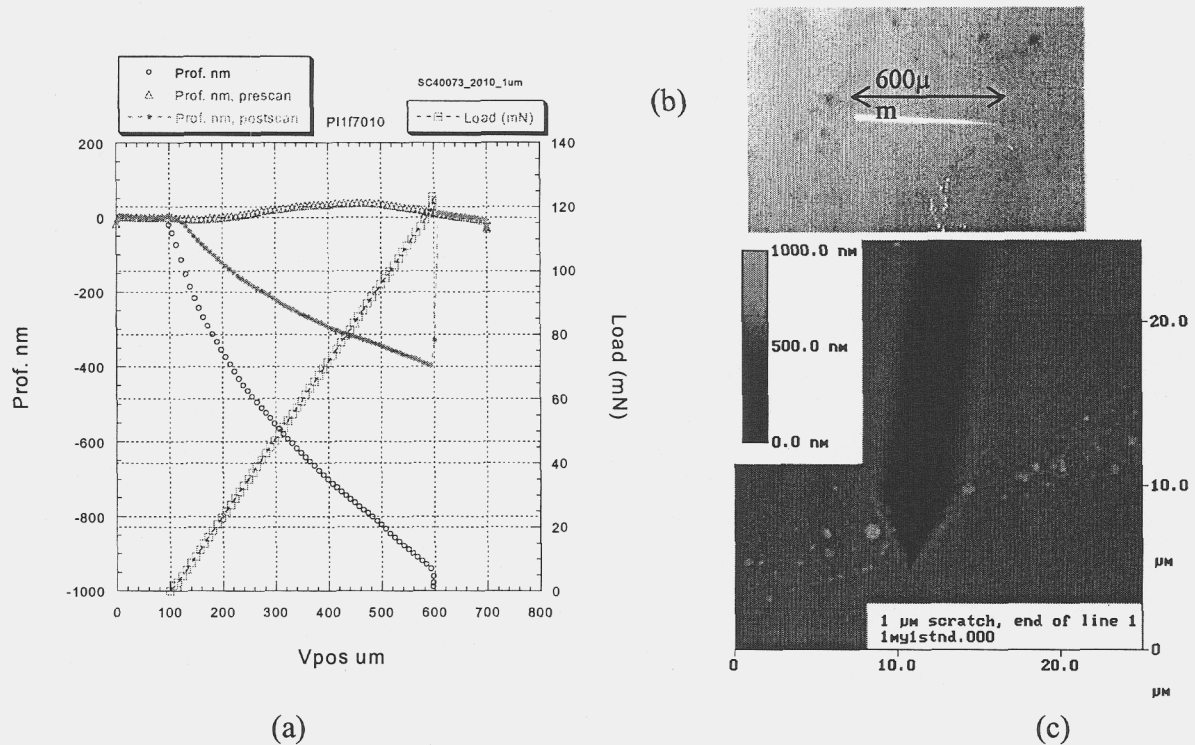


Figure 4. (a) Profiles before (triangles), during (open circles) and after scratching (filled circles), and loading data (open squares) for a one μm deep scratch. (b) optical micrograph of 1 micrometer deep scratch. (c) atomic force micrograph of the end-point of a one μm deep scratch.

3.0 RESULTS AND DISCUSSION

3.1 Embedded Gold Nanoparticle Defects

The results of the damage testing at the Zeus Facility (355 nm, 7.6 ns pulse, 10 Hz, ~ 15 s, S/1) are shown in table 1. Damage was detected by light scattering and Nomarski microscopy. Au particles on the surface had no effect on the damage threshold. A 100nm SiO_2 coating increased the apparent damage threshold. The key observation here is that damage was more facile on the 500nm SiO_2 coated 60nm Au particles than on the 100nm SiO_2 -coated 60nm Au particles. The damage morphology was that of point defects (see figure 5.).

Table 1. 355 nm, 7.6 ns damage testing of engineered Au particle sample. "Threshold" refers to damage observed by Nomarski microscopy at two micron resolution.

Sample	Orientation	Front "Threshold" (J/cm^2)	Rear "Threshold" (J/cm^2)
SC40077 (control)	60-nm Au particles no coating	9 ± 1 (Au particles)	7 ± 1 (bare)
SC40077 (control)	Bare etched substrate	7 ± 1 (bare)	7 ± 1 (Au particles)
SC40079	Side 1 incident (500nm)	< 0.7 (500nm)	> 17 (100nm)
SC40079	Side 2 incident (100nm)	19 ± 2 (100nm)	5 ± 1 (500nm)

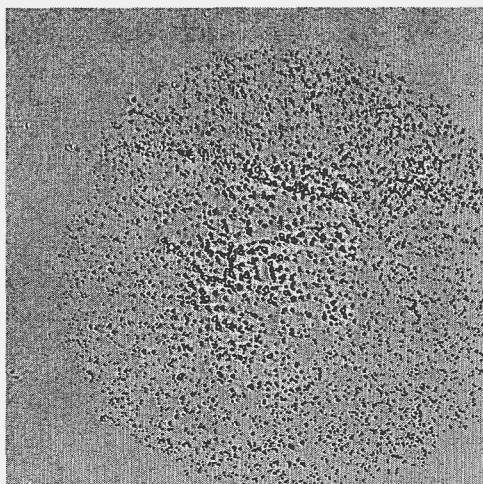


Figure 5. Light microscope image with background subtraction of a 10 J/cm^2 (355nm, 7.6 ns) single shot damage region. The sample is 60 nm Au particles with 500nm SiO_2 coating. The laser spot diameter is $700 \mu\text{m}$.

We can look at the damage morphology in more detail with atomic force microscopy (see figure 5). On the 500nm coated side at low fluence ($<5 \text{ J/cm}^2$ 7.6 ns pulse) the damage hole is asymmetric with a flat edge on only one side of the hole with a diameter of $\sim 1 \mu\text{m}$. The hole is 500nm deep, suggesting that the entire coating is removed but not the substrate. At higher fluence ($>5 \text{ J/cm}^2$) the hole shape is more symmetric and deeper ($\sim 700\text{nm}$). The hole profile has a kink in it suggesting more than one desorption process has occurred.

While damage testing in the Zeus facility suggests that there is a difference in front versus rear surface damage propensity, the atomic force microscope results could not discern a difference in front versus rear surface damage, i.e., damage morphology at the same fluence on the front or rear was similar.

For damage on the 100nm SiO_2 coated side, holes in the coating were not observed at fluence less than $\sim 7 \text{ J/cm}^2$. Rather blisters appeared (see figures 7). The protrusions on the laser-exposed area were higher (200nm) and wider than on the unexposed areas. The blisters suggest the apparent difference in the 355-nm laser damage threshold between the 500nm and 100nm coated sides can be attributed to the ability of the thinner coating to absorb some of the otherwise damaging energy via film deformation. The threshold for blister formation is not known; blisters were observed at all fluences tested less than 7 J/cm^2 .

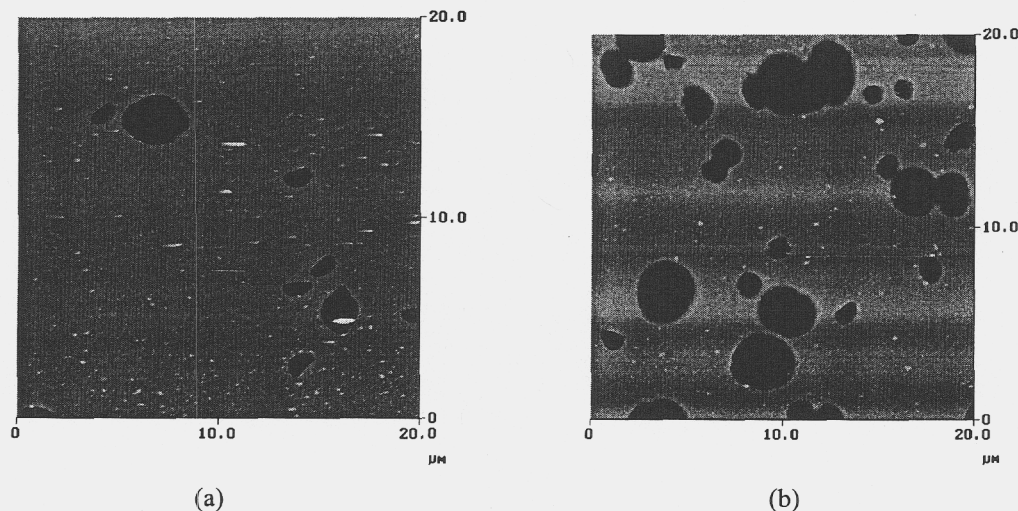


Figure 6. Atomic force image of point damage. Panel (a) is a top view of point damage at 0.7 J/cm^2 for 60nm Au particles on SESO substrate coated with 500nm SiO_2 . The color scale is 1000nm black to white. The observed holes are 500nm deep. Panel (b) is a top view of point damage at $7-8 \text{ J/cm}^2$ for 60nm Au particles on SESO substrate coated with 500nm SiO_2 . Black to white is 1600nm. The observed holes are 700nm deep.

At higher fluence point defect damage was observed with symmetric shape and $\sim 1 \mu\text{m}$ diameter and 250nm depth (see figure 7). In contrast no damage is reported at these fluences with light scattering and Nomarski microscopy on the Zeus facility. While the atomic force microscope can find the morphological changes that occur on the 100nm coated 60nm Au particles exposed to 3ω laser light, it is very difficult to discern changes with standard (light scattering and Nomarski microscopy) damage assessment techniques with fluences up to 17 J/cm^2 .

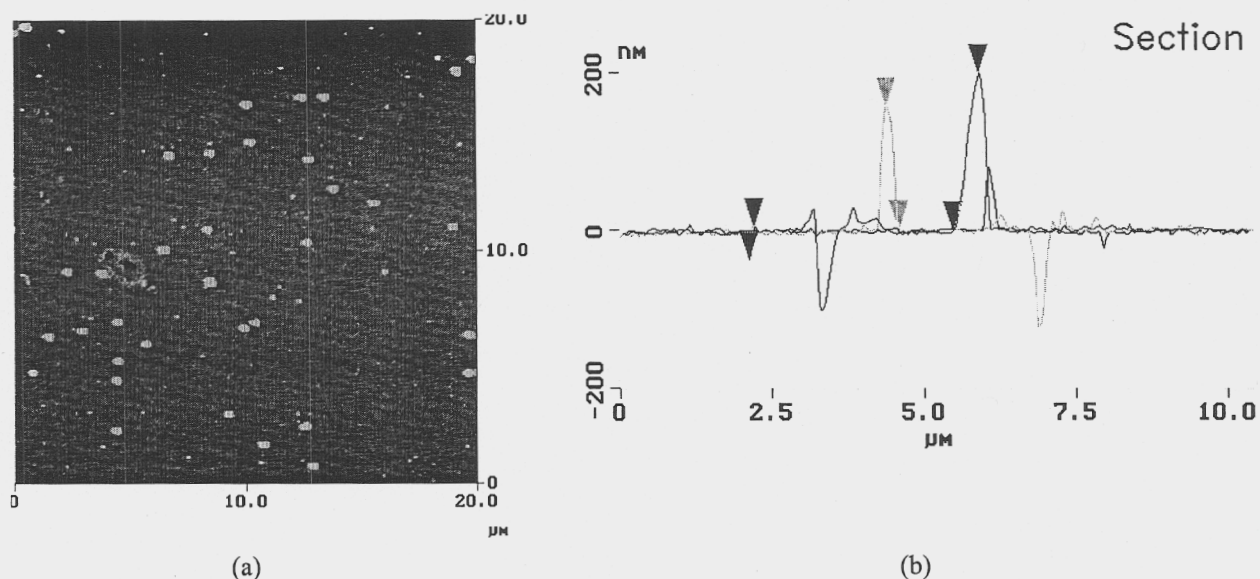


Figure 7. (a) AFM top view image of blisters formed on 60nm Au particle coated with 100nm of SiO_2 after exposure to 355nm 7.6 ns laser pulse at $\sim 5 \text{ J/cm}^2$ on laser input side. (b) cross section of 2 blisters showing 200nm height and $\sim 1 \mu\text{m}$ width.

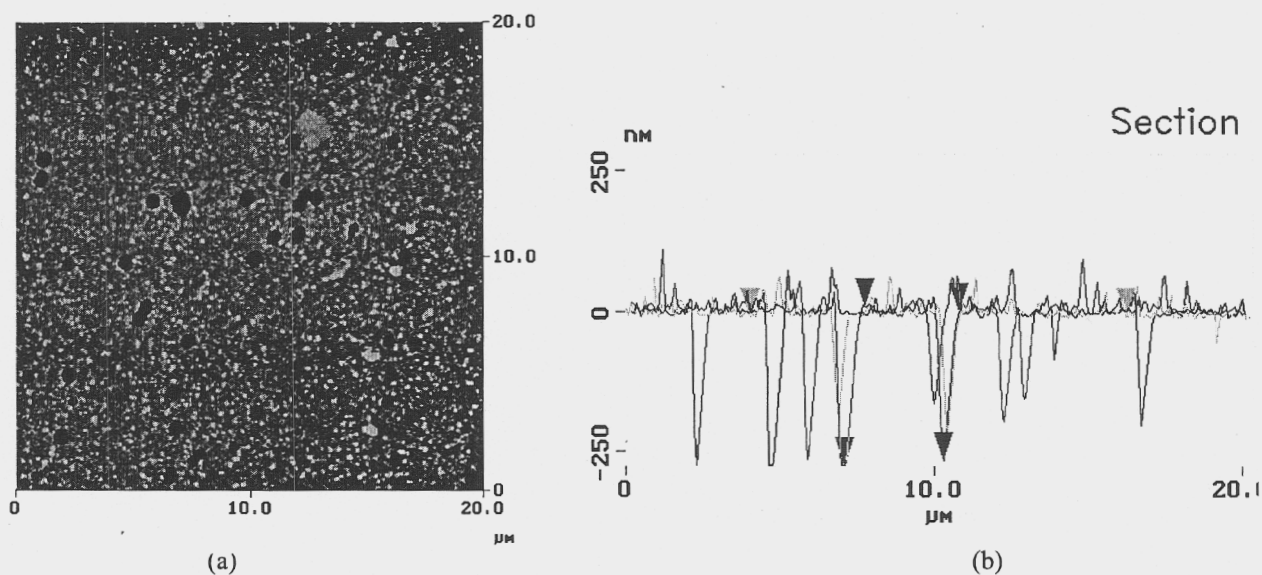


Figure 8. (a) AFM top view image of hole formed on 60nm Au particle coated with 100nm of SiO_2 after exposure to 355nm 7.6 ns laser pulse at $\sim 12 \text{ J/cm}^2$ on laser input side. (b) cross section of holes showing 250nm height and $\sim 1 \mu\text{m}$ width.

The uncoated etched SESO sample (no gold particles) produced no observable damage and no time-of-flight (TOF) desorption signal. This is presumably due to insufficient fluence on target in the Argonne facility. 355-nm damage and TOF desorption signal was observed for the 40nm Au particles coated with 500nm (see figures 9 and 10 below). The TOF signal can be characterized as desorption of the SiO_2 layer and fragments thereof. A significant Au desorption signal was observed without the post-ionization. This is observed in spite of the fact that the desorption laser has insufficient energy (3.5 eV) to ionize Au with a single photon. The post-ionization laser (Ti:sapphire $3h\nu + h\nu$) increased the sensitivity to the desorbed Au signal by a factor of 3 to 5, indicating neutral Au is also desorbed. Post-ionization laser tuned to Si (Ti:sapphire $2h\nu + 3h\nu$) revealed very little increase in Si signal due to post-ionization, indicating that little neutral Si is desorbed. This observation may be a characteristic of the SiO_2 fragmentation process. The damage morphology with the small laser beam spot and large laser beam spots were identical (see figure 10 and figure 6a).

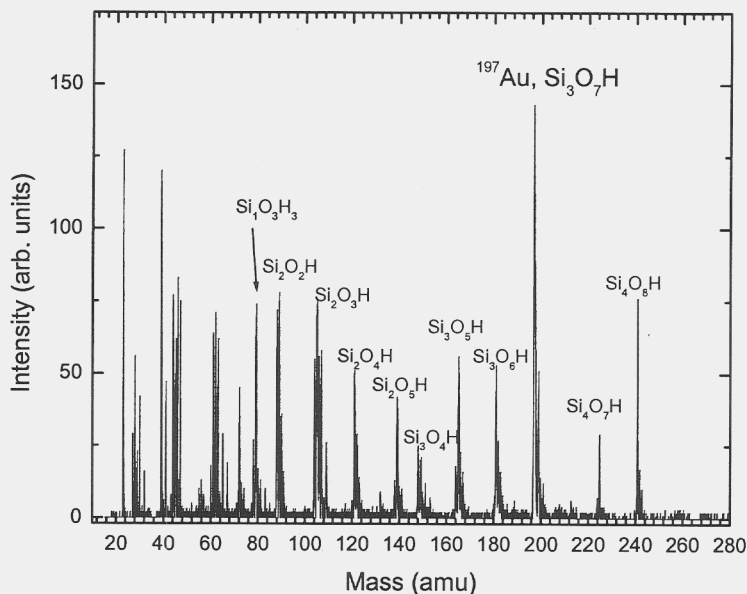


Figure 9. Time-of-flight of the laser desorbed material from 40nm gold particles sample with 500nm SiO_2 overcoat.

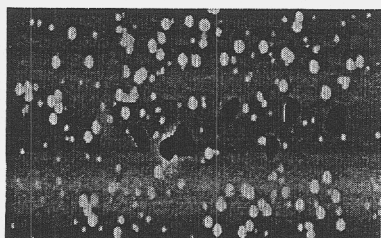


Figure 10. Atomic Force Microscopy of the Laser Damaged, 40nm gold particles sample with 500nm SiO_2 overcoat. Scale of the image is 15 μm from the left to right side.

According to estimates [see Rubenchik and Feit in this issue] the temperature on the surface of the gold nanoparticle reaches 3700°C for a fluence of 0.7 J/cm^2 and thermal conduction in the SiO_2 of $k=0.04 \text{ W/cm/K}$. This temperature is sufficient to start a thermal explosion. The final craters were about $1\text{-}\mu\text{m}$ size in agreement with estimates presented there. These experiments with crater formation many times larger than the initial nanoparticle confirms the pattern of damage induced by nanoparticles presented by Rubenchik and Feit. The model includes the formation and growth of a plasma fireball with storage of enough energy to produce the observed crater.

3.2 Mechanically Induced Defects

The mechanically engineered sample was damage tested at LLNL with the Zeus laser facility. The results of the damage testing at the Zeus Facility (355 nm, 7.6 ns pulse, 10 Hz, S/1, 700 μm spot diameter) are shown in figure 11

and 12. Damage was detected by light scattering and Nomarski microscopy. The indents and scratches were all tested with the mechanically induced damage on the laser exit side of the sample. Laser-induced damage thresholds were determined for each row of indents or scratches by exposing each site for up to 100 shots at a given fluence. Samples were inspected by microscope prior to and after laser exposure.

The damage threshold smoothly increased with decreasing indent depth from 13 μm to 2 μm . No damage at the 2- μm indent sites was observed at the fluences investigated; however, some front surface damage was observed at 35 J/cm^2 . The 2- μm indent had no cracking associated with the indent. Alternatively, the threshold penetration for non-plastic deformation is 5 μm .

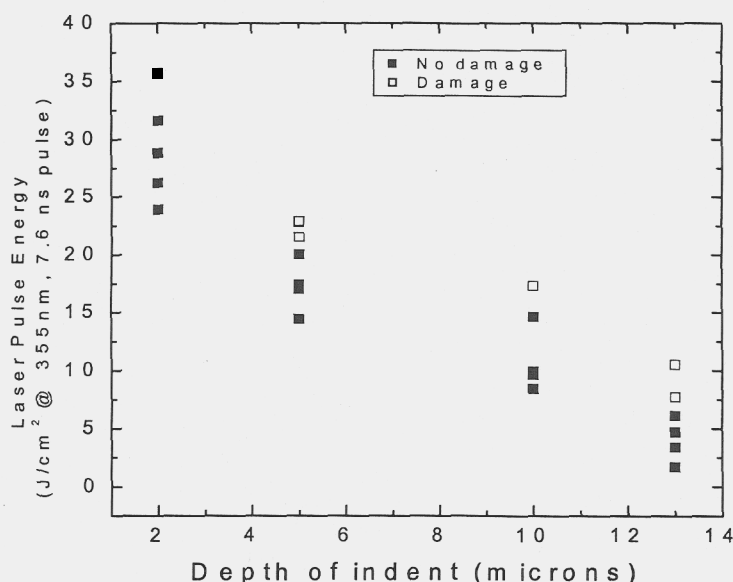


Figure 11. Plot of Zeus laser fluence (355nm, 7.6 ns pulse) versus indent depth with damage result for mechanical indents 2, 5, 10 and 13 μm in depth. Filled symbols represent multiple-shots-on-one-spot (S/1) results where no damage was observed by Nomarski microscopy after 100 shots at the plotted fluence. The open symbols represent S/1 results where damage was observed by Nomarski microscopy after 100 or less shots.

The damage threshold for scratches was lower than for indents at the same depth. 5- μm and 2- μm deep scratches showed cracking in the fused silica as well as deformation. Although there were only three 5- μm scratches to investigate, they damaged at relatively low fluence. The damage threshold for the 2- μm deep scratches was 5 J/cm^2 . There is a drastic change in the morphology before exposure to laser pulses of the 1- μm deep scratches compared with the 2- μm deep scratches. The 1- μm deep scratches show no signs of cracking. Only plastic deformation is observed in the 1 μm and shallower scratches (see figure 4). In coincidence with the change in morphology there is also a dramatic change in the damage threshold; there is a five-fold increase in the damage threshold for 1- μm scratches compared to 2- μm deep scratches. One of the most interesting observations is that damage on the scratches did not occur randomly along the scratch. Damage was always centered at the end of the scratch where the scratch was the deepest (see figure 13). The laser pulse during the damage test was always centered 150-200 μm from the deep end of the scratch along the scratch. The beam fluence only changed by about 5-10% over this region accounting for profile falloff and shot-to-shot wander. Essentially, the fluence was constant over the 200- μm range.

Scratches damage more readily than indents at the same depth. Plastic deformation without cracking does not lead to as serious a damage initiation problem as scratches with cracking. The plastic deformation leads to a densification of the fused silica³. The densified region has a higher index of refraction and can thus act as a means

of collecting light from the entire laser pulse and then concentrating it at the end of the scratch with the most densified material.

These observations may also help explain the damage growth of laser-damaged fused silica. Wong et al.⁸ have shown that the laser damaged region is densified by approximately 20%. Kubota et al.⁹ have calculated a similar densification for laser shocked silica. The densification and cracking in the laser damaged region leads to growth of the damage on subsequent shots, possibly via the collection of the light via the higher index of refraction for the densified region.

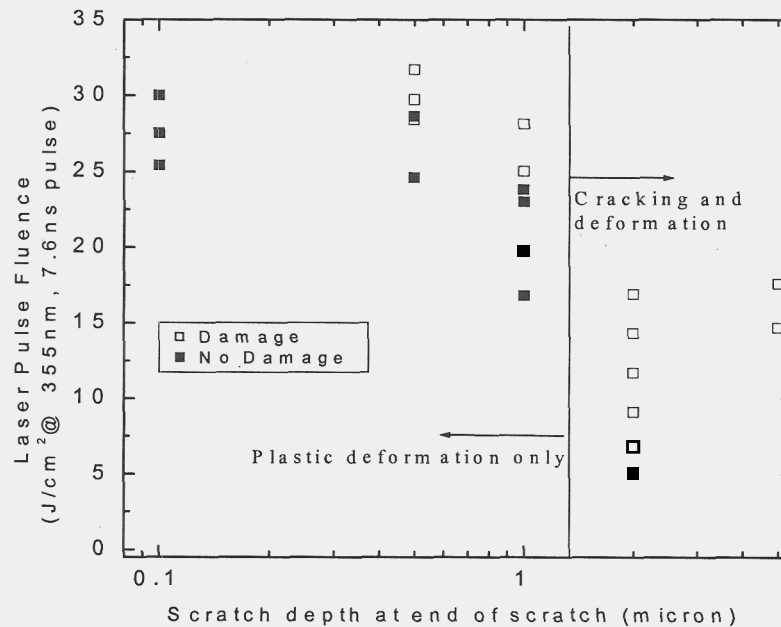


Figure 12. Plot of Zeus laser fluence (355 nm, 7.6 ns pulse) versus scratch depth with damage result for mechanical scratches 0.1, 0.5, 1, and 2 microns in depth. Filled symbols represent S/I results where no damage was observed by Nomarski microscopy after 100 shots at the plotted fluence. The open symbols represent S/I results where damage was observed with Nomarski microscopy after 100 or less shots.

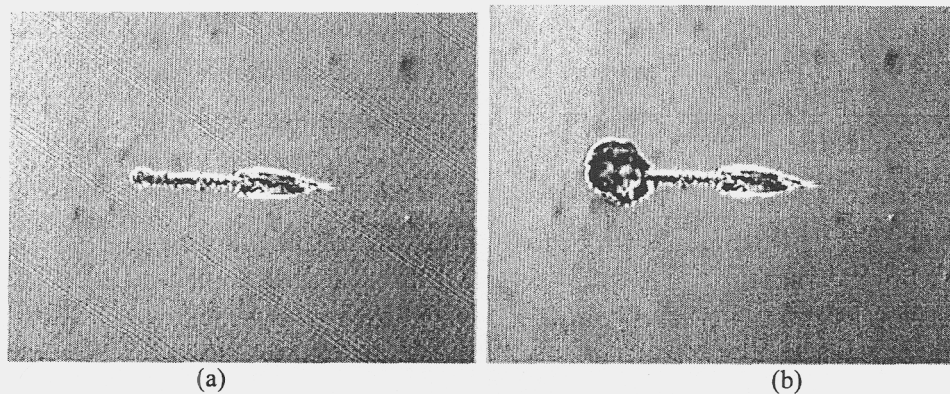


Figure 13. (a) 2 micron deep scratch morphology before laser exposure observed by Nomarski microscopy. (b) damage and scratch morphology after 30 shots at 9 J/cm². The initial scratch length is ~ 500 microns.

The presence of cracks can produce field enhancement both as a result of electrostatic enhancement pointed out by Blombergen¹⁰ and as interference of light reflected and scattered by cracks¹. Also, the cracks weaken the strength of material. The deposition of energy in the weakened material can also produce damage at lower laser fluence. Coupling cracks with densified material creates still lower threshold material. If polishing only covers over and fills in the region, lower threshold material may still remain.

4.0 CONCLUSIONS

The interaction of 355 nm laser light with engineered defects in fused silica is revealing the fundamental mechanisms of laser damage. Embedded gold nanoparticles are revealing the nature of point-defect initiated damage mechanisms; whereas, controlled scratches reveal mechanisms which enhance the laser fluence in the laser-solid interaction.

ACKNOWLEDGEMENTS

The authors wish to thank Gary Loomis for deposition of SiO₂ and Dino Ciarlo for deposition of Cr grounding grid for the CHARISMA measurements. This work was performed under the auspices of the U. S. Department of Energy at Lawrence Livermore National Laboratory under contract number W-7405-ENG-48.

REFERENCES

- [1] F. Y. Genin, A. Salleo, T. V. Pistor, and L. L. Chase, *Journal of The Optical Society of America A-Optics Image Science And Vision* **18**, 2607 (2001)
- [2] A. Salleo, F. Y. Genin, J. Yoshiyama, C. J. Stolz, and M. R. Kozlowski, "Laser-induced damage of fused silica at 355 nm initiated at scratches," in *Laser-Induced Damage in Optical Materials: 1997*, G. J. Exarhos, A. H. Guenther, M. R. Kozlowski, M. J. Soileau, Editors, SPIE Vol. **3244**, 341 (1998).
- [3] D. W. Camp, M. R. Kozlowski, L. M. Sheehan, M. Nichols, M. Dovik, R. Raether, and I. Thomas, "Subsurface damage and polishing compound affect the 355-nm laser damage threshold of fused silica surfaces," in *Laser-Induced Damage in Optical Materials: 1997*, G. J. Exarhos, A. H. Guenther, M. R. Kozlowski, M. J. Soileau, Editors, SPIE Vol. **3244**, 356 (1998).
- [4] M. D. Feit, J. Campbell, D. Faux, F. Y. Genin, M. R. Kozlowski, A. M. Rubenchik, R. Riddle, A. Salleo, and J. Yoshiyama, "Modeling of laser-induced surface cracks in silica at 355 nm," in *Laser-Induced Damage in Optical Materials: 1997*, G. J. Exarhos, A. H. Guenther, M. R. Kozlowski, M. J. Soileau, Editors, SPIE Vol. **3244**, 350 (1998).
- [5] S. Papernov, A. W. Schmid, R. Krishnan, and L. Tsybeskov, "Using colloidal gold nanoparticles for studies of laser interaction with defects in thin films," in *Laser-Induced Damage in Optical Materials: 2000*, G. J. Exarhos, A. H. Guenther, M. R. Kozlowski, K. L. Lewis, M. J. Soileau, Editors, SPIE Vol. **4347**, 146 (2001).
- [6] M. J. Pellin, C. E. Young, W. F. Calaway, J. E. Whitten, D. M. Gruen, J. D. Blum, I. D. Hutcheon, G. J. Wasserburg, *Philosophical Transactions Of The Royal Society Of London Series A-Mathematical Physical And Engineering Sciences* **333**, 133 (1990).
- [7] C. Z. Tan, J. Arndt, and H. S. Xie, *Physica B* **252**, 28 (1998).
- [8] J. Wong, D. Haupt, J. Kinney, J. Ferriere, I. Hutcheon, S. Demos, and M. Kozlowski, "Nature of damage in fused silica induced by high-fluence 3-omega 355-nm laser pulses, a multiscale morphology microstructure and defect chemistry study," in *Laser-Induced Damage in Optical Materials: 2000*, G. J. Exarhos, A. H. Guenther, M. R. Kozlowski, K. L. Lewis, M. J. Soileau, Editors, SPIE Vol. **4347**, 466. (2001).
- [9] A. Kubota, M. J. Caturla, J. S. Stolken, and M. D. Feit, "Densification of fused silica due to shock waves and its implications for 351 nm laser induced damage," *Optics Express* **8**, 611 (2001).
- [10] N. Blombergen, "Laser induced electric breakdown in solids," *IEEE J. of Quantum Electr.* **10**, 375 (1974).